CHAOS
Theory and Applications
in Applied Sciences and Engineering

e-ISSN: 2687-4539
RESEARCH ARTICLE
Vol.5 / No.4 / 2023 / pp.300-307
Special Issue
https://doi.org/10.51537/chaos.1324355

Weighted and Well-Balanced Nonlinear TV-Based Time-Dependent Model for Image Denoising

Alka Chauhan *,[1], **Santosh Kumar** *,[2] **and Khursheed Alam** *,[3]
*Department of Mathematics, Sharda School of Basic Sciences and Research, Sharda University Greater Noida-201310 UP, India.

ABSTRACT The partial differential equation (PDE)-based models are widely used to remove additive Gaussian white noise and preserve edges, and one of the most widely used methods is the total variation denoising algorithm. Total variation (TV) denoising algorithm-based time-dependent models have seen considerable success in the field of image-denoising and edge detection. TV denoising algorithm is based on that signals with spurious detail have a high total variation and reduction of unwanted signals to achieve noise-free images. It is a constrained optimization-type algorithm. The Lagrange multiplier and gradient descent method are used to solve the TV algorithm to reach the PDE-based time-dependent model. To eliminate additive noise and preserve edges, we investigate a class of weighted time-dependent model in this study. The proposed method is investigated in a well-balanced flow form that extends the time-dependent model with an adaptive fidelity element. Adaptive function is fusing into the regularization term of the classical time-dependent model which successfully enhances the intensity of the regularizer function. We maintain the ability of the time-dependent model without any oscillation effects. Furthermore, we want to prove the viscosity solution of our weighted and well-balanced time-dependent model, demonstrating its existence and uniqueness. The finite difference method is applied to discretize the nonlinear time-dependent models. The numerical results are expressed as a statistic known as the peak signal-to-noise ratio (PSNR) and structural similarity index metric (SSIM). Numerical experiments demonstrate that the proposed model yields good performance compared with the previous time-dependent model.

KEYWORDS
Partial differential equation
Total variation
Time dependent model
Weighted and well balanced
Image denoising
Image smoothing
Viscosity solution
Explicit scheme

INTRODUCTION

Noise degraded the visual quality of images, and image lost their significant features due to these random signals. An image becomes noisy during the acquisition, transmission, and processing steps. However, noise occurs randomly but sometimes it may be data dependent. Artifacts do not originate from the original images produced due to the noise. There are two types of noise additive noise and multiplicative noise. Additive noise are random signals that depend on the state of the system like Gaussian noise. Multiplicative noise is random signals that depend on the state of the system like speckle noise. Gaussian additive noise is added to the original signal during the acquisition of the image and this noise is distributed uniformly all over the image.

The additive noisy image as $u_0 : \Omega \to \mathbb{R}$, Ω is a bounded region of $\mathbb{R}^2$ and it can be defined as

$$u_0(x) = u(x) + n(x). \tag{1}$$

Here $u(x)$, $x \in \Omega$ signifies the true image, the noisy image represented by $u_0(x)$, and Gaussian white noise $n(x)$ which contains zero mean and σ^2 represent variance.

Rudin *et al.* (1992) for the first time, introduced total variation functional with static constraint to reduce the additive Gaussian white noise and edge preservation and can be represented by the ROF model. The total-variation-based model was impressive in the preservation of geometrical boundaries. The denoising problem can be seen as a minimization problem from a variational perspective. The minimization problem consists of two terms first

Manuscript received: 10 July 2023,
Revised: 4 September 2023,
Accepted: 6 September 2023.

[1]alkachauhan5490@gmail.com
[2]skykumar87@gmail.com (**Corresponding author**)
[3]khursheed.alam56@gmail.com

one measures the fidelity of the observed image; the second term is the regularizer parameter which is used to reduce the noise from the image. The Euler Lagrange multiplier and gradient descent method to steady state to ROF model for image denoising and edge detection. The fixed-point algorithm to optimize the energy functional was given by Vogel and Oman (1996) for image denoising. Chan *et al.* (1999) introduced a two-dimensional non-linear primal-dual algorithm for image restoration. They used the Tikhonov regularizer instead of the image gradient term in the time-dependent model. To overcome the computational difficulty of the term $\frac{\nabla u}{|\nabla u|}$ they replaced the denominator term by $\sqrt{|\nabla u|^2+\beta}$ in the time-dependent model, where β is a parameter. These models achieved better results in image denoising, but computational cost is high in the case of deblurring. Marquina and Osher (2000) introduced the time-dependent model for image restoration. They multiplied the magnitude of the gradient in the ROF model for image denoising and deblurring. They have discussed Roe's explicit scheme to check the convergence rate of their model. El-Shorbagy *et al.* (2023) presented an analysis of the general fractional derivative function with the Mittag-Leffler kernel and ABC operator at various fractional orders. Haidong *et al.* (2023) presented an analysis of the four-dimensional Chaotic system in consideration of the Mittag-Leffler kernel. XU *et al.* (2022) introduced a study of numerical analysis of a two-dimensional torus chaotic system with a power-law kernel. Qu *et al.* (2022) proposed a novel approach for solving the non-linear fractional order diffusion equation with the neural network method. A class of hyperbolic and parabolic models for image denoising and edge detection are proposed by Kumar and Alam (2021a,b).

Barcelos *et al.* (2005, 2003) proposed a nonlinear anisotropic parabolic model for the elimination of the noise and also discussed the well-balanced flow in the parabolic model. They have used an adaptive parameter to maintain the balance between the forcing term and data fidelity term in the anisotropic diffusion model. The improved image fidelity term for image denoising is proposed by Smolka (2008). Prasath and Vorotnikov (2014) generalized the PM model with a weighted and well-balanced flow equation and obtained better results comparatively. To make the PM model in terms of weighted and well-balanced, they used the diffusion function which depends on the magnitude of the image gradient and spatial variable. A weighted total variation-based model using mean curvature as a regularizer function was recently introduced by Phan (2020). They used the split Bergman method to obtain a fast convergence rate. Li and Li (2021) introduced a weighted total variation model using the exponential regularizer function. Many other researchers introduced the well-balanced model inspired by mean curvature motion and biased, see reference, (El-Fallah and Ford 1998; Chen *et al.* 1999).

In this study, we propose a weighted and well-balanced time-dependent model to minimize the energy functional by evolving the Euler-Lagrange equation. This model is related to a variational model with the diffusivity linked to the regularizer. The Charbonnier diffusivity is used in the time-dependent model, it is related to non-convex regularization (Charbonnier *et al.* 1994; Weickert 1997). An adaptive function ξ is fused in the regularizer term of the weighted and well-balanced time-dependent model. Experiments on many different gray-scale images are conducted to show the advantage of the weighted and well-balanced time-dependent model over the old model. Quantitative analysis shows that the proposed model is very effective and efficient in both noise reduction and edge detection. Furthermore, we want to prove the viscosity solution of a weighted and well-balanced time-dependent model.

This paper is organized as follows: The weighted and well-balanced denoising techniques are given in section 2. The viscosity solution of the weighted and well-balanced time-dependent model is given in section 3. The explicit scheme of the weighted and well-balanced model is given in section 4. In Section 5, the results are given in Figures 2-6, and Table 1, last, the conclusion is in Section 6.

TV-BASED WEIGHTED AND WELL-BALANCED TIME-DEPENDENT MODEL FOR DENOISING ALGORITHM

Rudin *et al.* (1992) introduced a TV-based regularisation functional for image denoising and edge detection. The restricted regularisation functional can be expressed as:

$$\text{minimize} \int_\Omega |\nabla u|\, dx = \int_\Omega \sqrt{u_x^2+u_y^2}\, dx, \tag{2}$$

$$\text{subject to } ||u-u_0||_{L^2}^2 = |\Omega|\sigma^2.$$

Using the definition of Euler-Lagrange and applying the equation (2). Then it can be expressed as:

$$0 = -\nabla.\left(\frac{\nabla u}{|\nabla u|}\right) + \lambda(u-u_0). \tag{3}$$

The value of $\nabla u = 0$ then the equation (3) is not well defined. Then the TV-based functional can be extended in another form:

$$\int_\Omega |\nabla u|_\gamma\, dx = \int_\Omega \sqrt{u_x^2+u_y^2+\gamma}\, dx. \tag{4}$$

Here $\gamma > 0$ as given in see reference (Chang and Chern 2003).

In the TV model diffusion takes place along the gradient orthogonal direction so that edges can be preserved during smoothing of the image. This model approximates the flat areas by considering the piece-wise constant surface and emerges the staircase artifacts. The equation (3) can be written as a time-dependent model given by (Rudin *et al.* 1992):

$$\frac{\partial u}{\partial t} = \nabla.\left(\frac{\nabla u}{|\nabla u|}\right) - \lambda(u-u_0), \tag{5}$$

with homogeneous Neumann boundary conditions $\frac{\partial u}{\partial \vec{n}} = 0$ and $u(x,0) = u_0(x)$ and scale parameter $\lambda > 0$. The left-hand side of the equation (5) is the regularization term that denotes the prior constraint and $(u-u_0)$ data fidelity term and λ is the Lagrange multiplier used to adjust the regularization term and data fidelity term. u_0 approaches u at a larger value of λ and the image lost its important details for a much larger value of λ.

The improved TV-based time-dependent model for image restoration is proposed by Marquina and Osher (2000):

$$\frac{\partial u}{\partial t} = |\nabla u|\nabla.\left(\frac{\nabla u}{|\nabla u|}\right) - |\nabla u|\lambda(u-u_0), \tag{6}$$

with the same boundary conditions above.

Gilboa *et al.* (2006) introduced the spatially adaptive balance term parameter λ and it can be made flexible. The well-balanced flow may also be further generalized. For instance, it is possible to make the diffusion coefficient depend on the picture u and the results in various diffusion flows and be constructed to have an impact on the restoration procedure. To extend the model (6) into weighted and well-balanced flow model:

$$\frac{\partial u}{\partial t} = \xi\,|\nabla u|\nabla.\left(\frac{\nabla u}{|\nabla u|}\right) - (1-\xi)|\nabla u|\lambda(u-u_0). \tag{7}$$

Here $\xi = \xi(|\nabla G_\sigma * u|)$, G_σ is represent as low pass filter or Gaussian kernel and $G_\sigma * u$ is a convolution and the diffusivity function ξ such as:

$$\xi(s) = \frac{1}{\sqrt{1+(|s|^2/K^2)}}, \tag{8}$$

where $\xi(s) \geq 0$ is a decreasing function and satisfying $\xi(0) = 1$ and $\xi(s) \to 0$ as $s \to \infty$ and K is the diffusivity parameter. It is related to the convex regularizer, see references (Charbonnier *et al.* 1994; Weickert 1997).

Motivated by Álvarez *et al.* (1992); Prasath and Vorotnikov (2014), we want to show the theoretical considerations and viscosity solution of the weighted and well-balanced time-dependent model as given in the next section.

THEORETICAL CONSIDERATIONS

We describe the mathematical formulation as the viscosity solution of the weighted and well-balanced time-dependent model (7). It can be written as:

$$\begin{aligned}\frac{\partial u}{\partial t} &= \xi(\nabla G_\sigma * u)a_{ij}(\nabla u)u_{x_ix_j} - \lambda|\nabla u|(1-\xi(\nabla G_\sigma * u))\\ &(u-u_0),\ x \in \mathbb{R}^2, t \in \mathbb{R}_+.\end{aligned} \tag{9}$$

Here

$$a_{ij}(p) = \delta_{ij} - \frac{p_i p_j}{|p|^2},$$

$$G_\sigma \in C^{1,1}(\mathbb{R}^2,\mathbb{R}),\ \ G_\sigma(p) > 0 \text{ for all } p \text{ in } \mathbb{R}^2, \tag{10}$$

and u_0 is continuous on $\mathbb{R}^2$.

The equation (9) represents the PDE-based diffusion equation with possible high degeneracy and a quasilinear term $a_{ij}(\nabla u)u_{x_ix_j}$, nonlocal term $\xi(\nabla G_\sigma * u)$ and data and fidelity term is $\lambda(1-\xi(\nabla G_\sigma * u))|\nabla u|(u-u_0)$.

Definition. A function u is a viscosity sub-supersolution of equation (9) from the space

$$u \in C(\mathbb{R}^2 \times [0,T]) \cap L^\infty(0,T;W^{1,\infty}(\mathbb{R}^2)) \tag{11}$$

if for any $\phi \in C^2(\mathbb{R}^2 \times \mathbb{R})$ and any point $(x_0,t_0) \in \mathbb{R}^2 \times (0,T]$ of local maxima/minima of the function $u-\phi$ has

$$\begin{aligned}&\frac{\partial \phi}{\partial t}(x_0,t_0) - \xi(\nabla G_\sigma * u(x_0,t_0))a_{ij}(\nabla\phi(x_0,t_0))\phi_{x_ix_j}(x_0,t_0)+\\ &\lambda(1-\xi(\nabla G_\sigma * u(x_0,t_0)))|\nabla\phi(x_0,t_0)|(u-u_0)(x_0,t_0) \leq 0,\\ &\text{if } \nabla\phi(x_0,t_0) \neq 0,\end{aligned} \tag{12}$$

$$\begin{aligned}&\frac{\partial \phi}{\partial t}(x_0,t_0) - \xi(\nabla G_\sigma * u(x_0,t_0))\limsup_{p\to 0} a_{ij}(p)\phi_{x_ix_j}(x_0,t_0) \leq 0,\\ &\text{if } \nabla\phi(x_0,t_0) = 0.\end{aligned} \tag{13}$$

The viscosity solution of function is a viscosity sub and super solution.

Theorem. (i) The equation (9) has a viscosity solution in class (11) for every $T > 0$. Moreover,

$$\inf_{\mathbb{R}^2} u_0 \leq u(x,t) \leq \sup_{\mathbb{R}^2} u_0.$$

(ii) For any two viscosity solution u and v of (9),

$$\sup_{0\leq t\leq T} ||u(x,t)-v(x,t)||_{L^\infty(\mathbb{R}^2)} \leq C||u_0-v_0||_{L^\infty(\mathbb{R}^2)}. \tag{14}$$

Here u_0 and v_0 are Lipschitz continuous functions in $\mathbb{R}^2$ for every positive T and C is positive constant.

Proof. The viscosity solution u which is satisfied the inequality such that

$$\inf_{\mathbb{R}^2} u_0 \leq u(x,t) \leq \sup_{\mathbb{R}^2} u_0, \qquad \text{on} \quad \mathbb{R}^2 \times \mathbb{R}_+. \tag{15}$$

We put $\phi = \sup_{\mathbb{R}^2} u_0 + \delta t(\delta > 0)$, then at the point (x_0,t_0), of the local maxima of $u-\phi$, (12) gives $\frac{\partial\phi}{\partial t}(x_0,t_0) \leq 0$ if $\nabla\phi(x_0,t_0) = 0$. So we get a contradiction $\frac{\partial\phi}{\partial t}(x_0,t_0) \equiv \delta > 0$ on $\mathbb{R}^2 \times [0,\infty)$.
attains a local maximum at (x_0,t_0) with $t_0 > 0$, then $\nabla\phi(x_0,t_0) = 0$ and from (12), $\frac{\partial\phi}{\partial t}(x_0,t_0) \leq 0$. This contradicts $\frac{\partial\phi}{\partial t}(x_0,t_0) \equiv \delta > 0$ on $\mathbb{R}^2 \times [0,\infty)$.
At $t_0 = 0$, the function $u-\phi$ have maximum value. So we can write
$u-\phi \leq \sup(u_0 - \sup_{\mathbb{R}^2} u_0)$, then $u \leq \sup_{\mathbb{R}^2} u_0 + \delta t$.
Similarly, we can write
$u \geq \inf_{\mathbb{R}^2} u_0 - \delta t$, as $\delta \to 0$, we can get (15).

In the starting, we demonstrate a uniform estimate for the equation (9).

$$||Du(t,.)||_{L^\infty(\mathbb{R}^2)} \leq e^{Ct}||Du_0||_{L^\infty(\mathbb{R}^2)}. \tag{16}$$

Here C is the constant number and it is depends on u_0, $\sup_{|p|\leq R}|\nabla^2 g_\epsilon(p)|$ and $\sup_p|a^\epsilon_{ij}(P)|$ with $R = ||w||_{L^\infty(\mathbb{R}^2)}||\nabla G||_{L^1(\mathbb{R}^2)}$.

Let u^ϵ be the smooth solution and it is given by

$$\begin{aligned}&\frac{\partial u^\epsilon}{\partial t} = \xi_\epsilon(\nabla G_\sigma * u^\epsilon)a^\epsilon_{ij}(\nabla u^\epsilon)u^\epsilon_{x_ix_j} -\\ &\lambda(1-\xi_\epsilon(\nabla G_\sigma * u^\epsilon))b^\epsilon(|\nabla u^\epsilon|)(u^\epsilon - u^\epsilon_0), \quad x \in \mathbb{R}^2, t \in \mathbb{R}_+,\\ &u^\epsilon(x,0) = u^\epsilon_0(x), \quad x \in \mathbb{R}^2.\end{aligned} \tag{17}$$

We establish an a priori estimate for ∇u. At that level, this estimate will become formal, and it will later be supported. In reality, we take a smooth solution concerning ϵ

$$\begin{aligned}&\frac{\partial u^\epsilon}{\partial t} = \xi_\epsilon(\nabla G_\sigma * w)a^\epsilon_{ij}(\nabla u^\epsilon)u^\epsilon_{x_ix_j} -\\ &\lambda(1-\xi_\epsilon(\nabla G_\sigma * u^\epsilon))b^\epsilon(|\nabla u^\epsilon|)(u^\epsilon - u^\epsilon_0), \quad x \in \mathbb{R}^2, t \in \mathbb{R}_+,\\ &u^\epsilon(x,0) = u^\epsilon_0(x), \quad x \in \mathbb{R}^2,\end{aligned} \tag{18}$$

where,

$$\begin{aligned}&0 < \epsilon < 1,\\ &a^\epsilon_{ij}(p) = (\epsilon+1)\delta_{ij} - \frac{p_i p_j}{|p|^2+\epsilon^2},\\ &b^\epsilon(p) = \sqrt{|p|^2+\epsilon},\ \ \xi_\epsilon = \xi+\epsilon,\ \ w \in L^\infty(\mathbb{R}^2 \times (0,\infty]),\end{aligned} \tag{19}$$

$u^\epsilon_0(x) \in C^\infty(\mathbb{R}^2)$ (antireflective) such that $u^\epsilon_0 \to u_0$ uniformly and $||\nabla u^\epsilon_0||_{L^\infty(\mathbb{R}^2)} \leq ||\nabla u_0||_{L^\infty(\mathbb{R}^2)}$ and u^ϵ_0 can be write $||u^\epsilon_0||_{L^\infty(\mathbb{R}^2)} \leq ||u_0||_{L^\infty(\mathbb{R}^2)}$.

The problems (17)-(19) admit a smooth solution $u^\epsilon \in C^\infty(\mathbb{R}^2 \times \mathbb{R}_+)$ by the definition of of the quasi-linear uniformly. According to equation (14), we can say that any smooth solution of a function is a

viscosity solution. For any positive number M and it is dependent on u_0, then it satisfies the condition $|u^\epsilon| \le M$.

The differentiating equation (18) w.r.to x_k, after that we multiplying $2u^\epsilon_{x_k}$, a summation w.r.to k is given by

$$\begin{aligned}
&\frac{\partial|\nabla u^\epsilon|^2}{\partial t} - \xi_\epsilon(\nabla G_\sigma * w)a^\epsilon_{ij}(\nabla u^\epsilon)\frac{\partial^2|\nabla u^\epsilon|^2}{\partial x_i \partial x_j} - \\
&\xi_\epsilon(\nabla G_\sigma * w)\frac{\partial a^\epsilon_{ij}}{\partial l}(\nabla u^\epsilon)u^\epsilon_{x_i x_j}\frac{\partial|\nabla u^\epsilon|^2}{\partial x_l} + \\
&\lambda\frac{\partial b^\epsilon(\nabla u^\epsilon)}{\partial m}(1-\xi_\epsilon(\nabla G_\sigma * w))(u^\epsilon - u^\epsilon_0)\frac{\partial|\nabla u^\epsilon|^2}{\partial x_m} \\
&= -2\xi_\epsilon(\nabla G_\sigma * w)a^\epsilon_{ij}(\nabla u^\epsilon)u^\epsilon_{x_k x_i}u^\epsilon_{x_k x_j} + \\
&2\frac{\partial\xi_\epsilon}{\partial l}(\nabla G_\sigma * w).(G_{\sigma x_l x_k} * w)a^\epsilon_{ij}(\nabla u^\epsilon)u^\epsilon_k u^\epsilon_{x_i x_j} - \\
&2\lambda b^\epsilon(\nabla u^\epsilon)(1-\xi)u^\epsilon_{x_k}u^\epsilon_{x_k} + 2\lambda b^\epsilon(\nabla u^\epsilon)(1-\xi)((u_0)^\epsilon_{x_k})u^\epsilon_{x_k} + \\
&2\lambda b^\epsilon(\nabla u^\epsilon)\nabla\xi(\nabla G_\sigma * u)\cdot\left(u * \frac{\partial\nabla G_\sigma}{\partial x_k}\right)(u-u_0)u_{x_k}.
\end{aligned} \tag{20}$$

From the definitions of a^ϵ_{ij}, b^ϵ, g^ϵ and h, we have

$$|a^\epsilon_{ij}(\nabla u^\epsilon)u^\epsilon_{x_i x_j}| \le C(a^\epsilon_{ij}(\nabla u^\epsilon)u^\epsilon_{x_k x_i}u^\epsilon_{x_k x_j})^{\frac{1}{2}}, \quad \sup_{\mathbb{R}^2} h \le C,$$

$$\sup_{\mathbb{R}^2}|Db^\epsilon(s)| \le C, \quad |G_{\sigma x_l x_k} * w| \le C,$$

$$|\frac{\partial\xi_\epsilon}{\partial l}(\nabla G_\sigma * w)| \le C(\xi_\epsilon(\nabla G_\sigma * w))^{\frac{1}{2}}.$$

Here C is a positive constant number and it is depend only $\sup|w|$, ξ_ϵ and M.

Using Cauchy's inequality the equation (20) estimates by

$$\begin{aligned}
&\frac{\partial|\nabla u^\epsilon|^2}{\partial t} - \xi_\epsilon(\nabla G_\sigma * w)a^\epsilon_{ij}(\nabla u^\epsilon)\frac{\partial^2|\nabla u^\epsilon|^2}{\partial x_i \partial x_j} - \\
&\xi_\epsilon(\nabla G_\sigma * w)\frac{\partial a^\epsilon_{ij}}{\partial l}(\nabla u^\epsilon)u^\epsilon_{x_i x_j}\frac{\partial|\nabla u^\epsilon|^2}{\partial x_l} \\
&+ \lambda\frac{\partial b^\epsilon(\nabla u^\epsilon)}{\partial m}(1-\xi_\epsilon(\nabla G_\sigma * w))(u^\epsilon - u^\epsilon_0)\frac{\partial|\nabla u^\epsilon|^2}{\partial x_m} \\
&\le C(|\nabla u^\epsilon|^2 + 1) \qquad \text{in } \mathbb{R}^2 \times \mathbb{R}_+.
\end{aligned} \tag{21}$$

Next, use the maximal principle (Brezis 1987) to deduce clearly (16). We just need to approximate (17), and we may get smooth solutions to draw this conclusion. Using the a priori estimate mentioned above, we get the valid approximate solutions.

Applying the maximization rule (Brezis 1987), the equation (21) yields $||\nabla u^\epsilon(.,t)||_{L^\infty(\mathbb{R}^2)} \le e^{Ct}$ we can defined $||\nabla(u_0)^\epsilon||_{L^\infty(\mathbb{R}^2)} \le e^{Ct}$ to reached to $||\nabla(u_0)||_{L^\infty(\mathbb{R}^2)} \le C_T$. This inequality can be reached to

$$|u^\epsilon(x,t) - u^\epsilon(y,t)| \le C_T|x-y|,$$

it is satisfy for every $x, y \in \mathbb{R}^2$, for all $t \in [0,T]$ and C_T represent the independent constant parameters it is depend on ϵ, t, x, y. Now for every $x \in \mathbb{R}^2$ and $s,t \in [0,T]$. A similar argument has led us to

$$|u^\epsilon(x,s) - u^\epsilon(x,t)| \le C_T|s-t|^{\frac{1}{2}}.$$

Using the Ascoli-Arzela theorem, a subsequence u^{ϵ_k} of u^ϵ exists, then

$$u^{\epsilon_k} \to u \quad as \quad \epsilon_k \to 0, \tag{22}$$

is locally uniformly. So easily get the inequality (16).

Second, we'll demonstrate the presence of a viscosity solution. From equation (22), we can say that u is the viscosity solution of the weighted and well-balanced model (9) in the sense of equations (12)-(13). Let $\phi \in C^2(\mathbb{R}^2 \times \mathbb{R}_+)$ be the result. Initially, we suppose that for a location $(x_0,t_0) \in \mathbb{R}^2 \times \mathbb{R}_+$ has a strict local maximum. When $u^{\epsilon_k} \to u$ is consistently close to (x_0,t_0), There is a local maximum for $u-\phi$ at the position (x_k,t_k) with

.

$$(x_k,t_k) \to (x_0,t_0), \quad k \to \infty \tag{23}$$

and

$$\nabla u^{\epsilon_k} = \nabla\phi, \quad \frac{\partial u^{\epsilon_k}}{\partial t} = \frac{\partial\phi}{\partial t}, \quad a^{\epsilon_k}_{ij}(\nabla u^{\epsilon_k})u^{\epsilon_k}_{x_i x_j} \le a^{\epsilon_k}_{ij}(\nabla\phi)\phi_{x_i x_j}.$$

Therefore, (17) implies that at (x_k,t_k),

$$\begin{aligned}
&\frac{\partial\phi}{\partial t} - \xi_{\epsilon_k}(\nabla G_\sigma * u^{\epsilon_k})a^{\epsilon_k}_{ij}(\nabla\phi)\phi_{x_i x_j} + \\
&b^{\epsilon_k}(\nabla\phi)(1-\xi_{\epsilon_k}(\nabla G_\sigma * u^{\epsilon_k}))(u^{\epsilon_k} - (u^{\epsilon_k}_0)) \le 0.
\end{aligned} \tag{24}$$

(1) If $\nabla\phi(x_0,t_0) \ne 0$, according to (23), $\nabla\phi(x_k,t_k) \ne 0$ for largest value of k and applying the limits to (24), we get

$$\begin{aligned}
&\frac{\partial\phi}{\partial t} - \xi(\nabla G_\sigma * u)a_{ij}(\nabla\phi)\phi_{x_i x_j} + \\
&b(\nabla\phi)(1-\xi(\nabla G_\sigma * u))(u-(u_0)) \le 0, \ \text{ at } (x_0,t_0),
\end{aligned} \tag{25}$$

It is similar to equation (9).
(2) If $\nabla\phi(x_0,t_0) = 0$, according to (23), $\nabla\phi(x_k,t_k) \to 0, \epsilon \to 0$ as $k \to 0$. The equation (24) reached to another form

$$\begin{aligned}
&\frac{\partial\phi}{\partial t} - (\xi(\nabla G_\sigma * u) + \epsilon_k)\left((\epsilon_k+1)\delta_{ij} - \frac{(\nabla\phi)_i(\nabla\phi)_j}{|\nabla\phi|^2+\epsilon^2}\right)\phi_{x_i x_j} \\
&\quad + b^{\epsilon_k}(\nabla\phi)(1-\xi(\nabla G_\sigma * u))(u^{\epsilon_k} - (u^{\epsilon_k}_0)) \le 0, \ \text{ at } (x_k,t_k).
\end{aligned} \tag{26}$$

If $b^{\epsilon_k}(\nabla\phi(x_k,t_k)) \to 0$ to (26), we get

$$\frac{\partial\phi}{\partial t} - \xi(\nabla G_\sigma * u)\left(\delta_{ij} - \frac{(\nabla\phi)_i(\nabla\phi)_j}{|\nabla\phi|^2+\epsilon^2}\right)\phi_{x_i x_j} \le 0, \ \text{ at } (x_0,t_0).$$

If $u-\phi$ has a local maximum at (x_0,t_0). The method of proof is consistent i.e., u is a sub-solution of (13). Similarly, it can be proven that u is a super-solution. Hence, u is a viscosity solution of (9).

.

DISCRETE SCHEME

The explicit scheme of the time dependent models (6) and (7):

$$\begin{aligned}
u_t = &\frac{u_{xx}(u_y^2+\gamma) - 2u_{xy}u_x u_y + u_{yy}(u_x^2+\gamma)}{(u_x^2+u_y^2+\gamma)} - \\
&\sqrt{u_x^2+u_y^2+\gamma}\,\lambda(u-u_0).
\end{aligned} \tag{27}$$

$$\begin{aligned}
u_t = \xi\,&\frac{u_{xx}(u_y^2+\gamma) - 2u_{xy}u_x u_y + u_{yy}(u_x^2+\gamma)}{(u_x^2+u_y^2+\gamma)} - \\
&(1-\xi)\sqrt{u_x^2+u_y^2+\gamma}\,\lambda(u-u_0).
\end{aligned} \tag{28}$$

We define the derivative terms as,

$$u^x_{ij} = \frac{u^n_{i+1,j} - u^n_{i-1,j}}{2\Delta x}; \quad u^y_{ij} = \frac{u^n_{i,j+1} - u^n_{i,j-1}}{2\Delta x};$$

$$u_{ij}^{xx} = \frac{u_{i+1,j}^n - 2u_{i,j}^n + u_{i-1,j}^n}{\Delta x^2}; \quad u_{ij}^{yy} = \frac{u_{i,j+1}^n - 2u_{i,j}^n + u_{i,j-1}^n}{\Delta x^2};$$

$$u_{ij}^{xy} = \frac{u_{i+1,j+1}^n - u_{i-1,j+1}^n - u_{i+1,j-1}^n + u_{i-1,j-1}^n}{4\Delta x \Delta x}; \quad u_{ij}^t = \frac{u_{i,j}^{n+1} - u_{i,j}^n}{\Delta t}.$$

Here u_{ij}^n is the approximation value of $u(x_i, y_j, t_n)$, $x_i = i\Delta x$, $y_j = j\Delta x$, $i, j = 1, 2, ..., N$, Δx spatial step and $t_n = n\Delta t$, $n \geq 1$, Δt is the time step size.

Let

$$r_{ij}^n = u_{ij}^{xx}((u_{ij}^y)^2 + \gamma) - 2u_{ij}^{xy}u_{ij}^x u_{ij}^y + u_{ij}^{yy}((u_{ij}^x)^2 + \gamma), \tag{29}$$

and

$$p_{ij}^n = ((u_{ij}^x)^2 + (u_{ij}^y)^2 + \gamma). \tag{30}$$

Then (27) reads as follows:

$$u_{ij}^t = \frac{r_{ij}^n}{p_{ij}^n} - \sqrt{((u_{ij}^x)^2 + (u_{ij}^y)^2 + \gamma)}\ \lambda\ (u_{ij}^n - u_{ij}^0). \tag{31}$$

Then (28) reads as follows:

$$u_{ij}^t = \xi_{ij}\ \frac{r_{ij}^n}{p_{ij}^n} - (1 - \xi_{ij})\sqrt{((u_{ij}^x)^2 + (u_{ij}^y)^2 + \gamma)}\ \lambda\ (u_{ij}^n - u_{ij}^0). \tag{32}$$

The function $\xi(|\nabla u|^2)$ can be discretised by,

$$\xi_{ij}^n = \psi'\left(\left(\frac{u_{i+1,j}^n - u_{i-1,j}^n}{\Delta x}\right)^2 + \left(\frac{u_{i,j+1}^n - u_{i,j-1}^n}{\Delta x}\right)^2\right).$$

For $\frac{\Delta t}{\Delta x^2} \leq 0.5$, the explicit technique is stable and convergent (Lapidus and Pinder 1983).

NUMERICAL EXPERIMENTS

The weighted and well-balanced time-dependent model for removing additive noise and preserving edges is proposed and applied to many 2-dimensional noisy grayscale images with different levels of noise parameters, we get the smooth images for denoising techniques. The original grayscale images of the size 256×256 with pixel values of [0, 255] such as Lena images, Boat images, and Figure 4(a). For numerical experiments, firstly to reduce the intensities of images lies in [0, 1]. To add the noise, we use the function imnoise (I, 'Gaussian', M, σ^2) in Matlab [MATLAB, 2022 version 9.12.0 (R2022a)], σ^2, and M are variance and mean zero respectively. The parameters $K = 5$ and $\lambda = 0.85$ are used in our numerical experiments (Catté *et al.* 1992; Chan *et al.* 1999).

We'll utilize the PSNR as a criterion for restoration which can be defined as:

$$\text{PSNR} = 10\log_{10}\left(\frac{R^2}{\frac{1}{mn}\sum_{i,j}^n (u_{i,j} - x_{i,j})^2}\right), \tag{33}$$

where $\{u_{i,j} - x_{i,j}\}$ are the differences in the pixel values between the original and denoised images. R is the maximum pixel value of the images.

The structural similarity index metric (SSIM) is used to compare the contrast and structure of the denoised image to the original image. The SSIM is formulated as:

$$\text{SSIM}(x, y) = \frac{(2 \times \mu_x\mu_y + D1) \times (2 \times \sigma_{xy} + D2)}{(\mu_x^2 + \mu_y^2 + D1)(\sigma_x^2 + \sigma_y^2 + D2)}, \tag{34}$$

where μ_x and μ_y are the mean of x and y, respectively, and x and y represent the local windows of the original image and denoised image, respectively. σ_{xy} denotes the covariance of x and y. $D1$=$(0.01 \times L)^2$ and $D2$=$(0.03 \times L)^2$ where L is the dynamic range of pixel values. SSIM value lies between 0 and 1. The higher value of SSIM gives a good visual quality of the denoised image and the lower value presents a poor visual quality of denoised image.

The proposed model is compared to a time-dependent model based on removing additive noise from the literature. Figure 1 represents the original Lena and Boat images. Figure 2(a-c) represents the noisy Lena images with ($\sigma^2 = 0.006, 0.008, 0.010$) respectively. Figure 2(d-f) represents the denoised images by the model (6) and Figure 2(g-i) represents the denoised images by the model (7). Figure 3(a-c) represents the noisy Boat images with ($\sigma^2 = 0.006, 0.008, 0.010$) respectively. Figure 3(d-f) represents the denoised images by the model (6) and Figure 3(g-i) represents the denoised images by the model (7). The numerical results are given in Figure 2-6 and Table 1 and achieve higher PSNR values by a weighted and well-balanced time-dependent model corresponding to the old model. The numerical results confirm that a weighted and well-balanced time-dependent model is very efficient in obtaining the solution.

(a) (b)

Figure 1 (a-b) Left side original Lena image and right side original Boat image.

(a) (b) (c) (d) (e) (f) (g) (h) (i)

Figure 2 (a-c) Noisy images with ($\sigma^2 = 0.006, 0.008, 0.010$); (d-f) corresponding denoised image by(6); (g-i) Denoised image by(7) respectively.

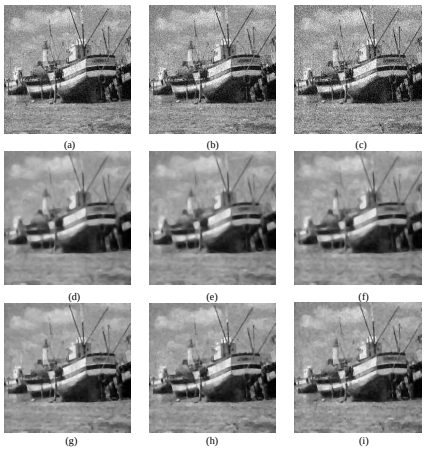

Figure 3 (a-c) Noisy images with ($\sigma^2 = 0.006, 0.008, 0.010$); (d-f) corresponding denoised image by (6); (g-i) Denoised image by (7) respectively.

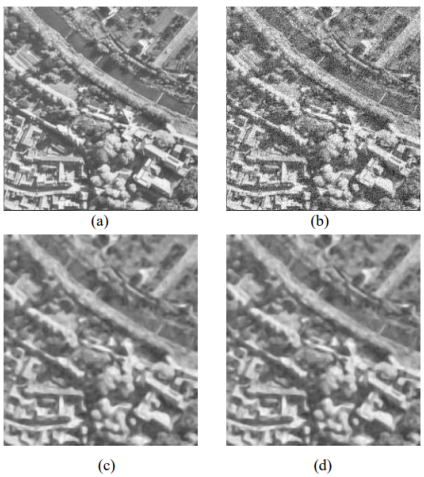

Figure 4 (a) Represent the original image; (b) Noisy image with $\sigma^2 = 0.010$ with PSNR and SSIM values are 20.13 and 0.6147 respectively; (c) Corresponding denoised image by model (6) with PSNR and SSIM values are 22.26 and 0.6825 respectively, at 5 iteration numbers; (d) Corresponding denoised image by model (7) with PSNR and SSIM values are 23.68 and 0.7769 respectively, at 5 iteration numbers.

Table 1 The comparison results.

Image	PSNR of noisy image	SSIM of noisy image	PSNR by (6)	SSIM by (6)	PSNR by (7)	SSIM by (7)
$\sigma^2 = 0.006$	22.41	0.4731	25.31	0.7645	28.15	0.8136
Lena $\sigma^2 = 0.008$	21.16	0.4274	25.19	0.7543	27.74	0.7943
$\sigma^2 = 0.010$	20.27	0.3914	25.08	0.7454	27.22	0.7743
$\sigma^2 = 0.006$	22.32	0.4566	24.24	0.6839	27.20	0.7725
Boat $\sigma^2 = 0.008$	21.06	0.4454	24.20	0.6735	26.89	0.7590
$\sigma^2 = 0.010$	20.17	0.4059	24.07	0.6633	26.56	0.7401
No. of iterations			10		10	

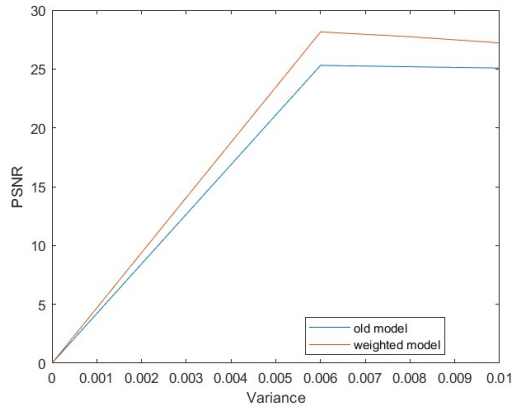

Figure 5 This graph is represented by Lena images, the results are given in terms of PSNR values in Table 1 for the weighted and well-balanced time-dependent model and the old model.

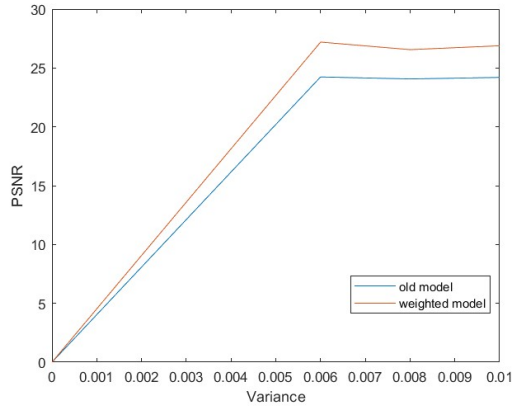

Figure 6 This graph is represented by Boat images, the results are given in terms of PSNR values in Table 1 for the weighted and well-balanced time-dependent model and the old model

CONCLUSION

In this paper, we proposed a total variation-based weighted and well-balanced time-dependent model for additive white noise reduction and preserved edges. The total-variation algorithm-based time-dependent model performs a good trade between noise reduction and edge preservation. A weighted function ξ is incorporated into the regularizer term of the time-dependent model to make it more effective and efficient for image denoising. The finite difference method is used to discretize the proposed model. To check the performance of the denoised images, we used the peak signal-to-noise ratio (PSNR) and structural similarity index metric (SSIM). The larger values of PSNR and SSIM present better results. Our model contains the larger PSNR and SSIM values corresponding to the old model. So the weighted and well-balanced time-dependent model improves the quality of the denoised images as well as better edges preserved corresponding to the old model at the same iteration numbers. The proposed model may be applied to image problems, such as deblurring, image segmentation, etc.

Availability of data and material

Not applicable.

Conflicts of interest

The authors declare that there is no conflict of interest regarding the publication of this paper.

Ethical standard

The authors have no relevant financial or non-financial interests to disclose.

LITERATURE CITED

Álvarez, L., P.-L. Lions, and J.-M. Morel, 1992 Image selective smoothing and edge detection by nonlinear diffusion. ii. SIAM Journal on Numerical Analysis **29**: 845–866.

Barcelos, C., M. Boaventura, and E. Silva, 2003 A well-balanced flow equation for noise removal and edge detection. IEEE Transactions on Image Processing **12**: 751–763.

Barcelos, C. A. Z., M. Boaventura, and E. C. Silva, 2005 Edge detection and noise removal by use of a partial differential equation with automatic selection of parameters. Computational & Applied Mathematics **24**: 131–150.

Brezis, H., 1987 *Analyse Fonctionnelle: Theorie et Applications*. Masson, Paris, 1987 (2e Tirage).

Catté, F., P. Lions, J. Morel, and T. Coll, 1992 Image selective smoothing and edge detection by nonlinear diffusion*. SIAM J. Numer. Anal. **29**: 182–193.

Chan, T. F., G. H. Golub, and P. Mulet, 1999 A nonlinear primal-dual method for total variation-based image restoration. SIAM J. Sci. Comput. **20**: 1964–1977.

Chang, Q. and I.-L. Chern, 2003 Acceleration methods for total variation-based image denoising. SIAM Journal on Scientific Computing **25**: 982–994.

Charbonnier, P., L. Blanc-Féraud, G. Aubert, and M. Barlaud, 1994 Two deterministic half-quadratic regularization algorithms for computed imaging. Proceedings of 1st International Conference on Image Processing **2**: 168–172 vol.2.

Chen, Y.-G., Y. Giga, and S. Goto, 1999 pp. 375–412 in *Uniqueness and Existence of Viscosity Solutions of Generalized mean Curvature Flow Equations*, edited by Ball, J. M., D. Kinderlehrer, P. Podio-Guidugli, and M. Slemrod, Springer Berlin Heidelberg.

El-Fallah, A. I. and G. E. Ford, 1998 On mean curvature diffusion in nonlinear image filtering. Pattern Recognition Letters **19**: 433–437.

El-Shorbagy, M. A., M. u. Rahman, and Y. Karaca, 2023 A computational analysis fractional complex-order values by abc operator and mittag-leffler kernel modeling. Fractals **0**: null.

Gilboa, G., N. Sochen, and Y. Zeevi, 2006 Variational denoising of partly textured images by spatially varying constraints. IEEE Transactions on Image Processing **15**: 2281–2289.

Haidong, Q., M. ur Rahman, S. E. Al Hazmi, M. F. Yassen, S. Salahshour, *et al.*, 2023 Analysis of non-equilibrium 4d dynamical system with fractal fractional mittag-leffler kernel. Engineering Science and Technology, an International Journal **37**: 101319.

Kumar, S. and K. Alam, 2021a A new class of nonlinear hyperbolic-parabolic model for image denoising with forward-backward diffusivity. Mathematics in Engineering, Science & Aerospace **12**: 435–441.

Kumar, S. and K. Alam, 2021b Pde-based hyperbolic-parabolic model for image denoising with forward-backward diffusivity. Computational Methods for Differential Equations **9**: 1100–1108.

Lapidus, L. and G. F. Pinder, 1983 Numerical solution of partial differential equations in science and engineering. SIAM Review **25**: 581–582.

Li, M.-M. and B.-Z. Li, 2021 A novel weighted total variation model for image denoising. IET Image Processing **15**: 2749–2760.

Marquina, A. and S. Osher, 2000 Explicit algorithms for a new time dependent model based on level set motion for nonlinear deblurring and noise removal. SIAM Journal on Scientific Computing **22**: 387–405.

Phan, T. D. K., 2020 A weighted total variation based image denoising model using mean curvature. Optik **217**: 164940.

Prasath, V. B. S. and D. Vorotnikov, 2014 Weighted and well-balanced anisotropic diffusion scheme for image denoising and restoration. Nonlinear Analysis-real World Applications **17**: 33–46.

Qu, H.-D., X. Liu, X. Lu, M. ur Rahman, and Z.-H. She, 2022 Neural network method for solving nonlinear fractional advection-diffusion equation with spatiotemporal variable-order. Chaos, Solitons & Fractals **156**: 111856.

Rudin, L. I., S. Osher, and E. Fatemi, 1992 Nonlinear total variation based noise removal algorithms. Physica D: Nonlinear Phenomena **60**: 259–268.

Smolka, B., 2008 Modified biased anisotropic diffusion processing of noisy color images. In *2008 9th International Conference on Signal Processing*, pp. 777–780.

Vogel, C. R. and M. E. Oman, 1996 Iterative methods for total variation denoising. SIAM Journal on Scientific Computing **17**: 227–238.

Weickert, J., 1997 A review of nonlinear diffusion filtering. In *Scale-Space Theory in Computer Vision*, edited by B. ter Haar Romeny, L. Florack, J. Koenderink, and M. Viergever, pp. 1–28, Berlin, Heidelberg, Springer Berlin Heidelberg.

XU, C., M. UR RAHMAN, B. FATIMA, and Y. KARACA, 2022 Theoretical and numerical investigation of complexities in fractional-order chaotic system having torus attractors. Fractals **30**: 2250164.

How to cite this article: Chauhan, A., Kumar, S., and Alam, K. Weighted and Well-Balanced Nonlinear TV-Based Time-Dependent Model for Image Denoising. *Chaos Theory and Applications*, 5(4), 300-307, 2023.